water

MDPI

Article

Enhancing Shear Strength of Weakly Consolidated Mudstone in Water-Diversion Tunnels Through Artificial Ground-Freezing Techniques: An Experimental and Theoretical Study

Hongmei Quan [1], Wenzhi Zhang [2], Junjie Li [3,*], Xiaoxue Ru [3], Jingbo Zhou [4] and Ran An [5]

[1] Lanzhou City University, Lanzhou 730070, China; qhm@lzcu.edu.cn
[2] Qiantang River Administration Design Institute Co., Ltd. of Zhejiang Province, Hangzhou 310016, China; onfdqpoh@moert.online
[3] Zhejiang Design Institute of Water Conservancy & Hydroelectric Power Co., Ltd., Hangzhou 310002, China; rxx8912@mail.zdwp.net
[4] Zhejiang Engineering Survey and Design Institute Group Co., Ltd., Ningbo 315031, China; yctovten@ousse.online
[5] Department of Civil Engineering, University of Bristol, Bristol BS8 1TR, UK; anran@wust.edu.cn
* Correspondence: ljj8903@mail.zdwp.net; Tel.: +86-13-7381-43465

Abstract: The utilization of artificial ground-freezing techniques is increasingly prevalent in the construction of water-diversion tunnels. The inadequate mechanical properties of weakly consolidated mudstone (WCM) pose significant challenges for tunneling construction. In this study, a series of triaxial shear tests were conducted on frozen specimens of WCM to elucidate its shear strength characteristics. The experiment involved four freezing temperatures (0, −5, −10, and −20 °C) and four confining pressures (1, 2, 3, and 4 MPa). The results indicate that the shear failure mode of the WCM exhibits distinct shear zone failure characteristics under artificial freezing conditions, particularly prominent in the lower temperature environments. As the freezing temperature gradually decreases, there is a substantial increase of over 200% in the shear strength of frozen specimens, accompanied by a corresponding decrease in yield strain. Furthermore, the cohesion and internal friction angle of frozen WCM increase as the freezing temperature decreases, following a complex exponential function relationship rather than a linear one. As the freezing temperature decreases from 0 °C to −20 °C, there is an increase in cohesion and internal friction angle from 1012 kPa to 1425 kPa, accompanied by a rise in the internal friction angle from 43.2° to 58.1°. Notably, the application of confining pressure exerts a pronounced influence on the shear strength of frozen WCM, with elevated levels of confining pressure resulting in a substantial augmentation of the shear strength. The failure mode of frozen WCM is significantly influenced by freezing temperatures. At low temperatures, the specimen of mudstone exhibits a shear failure behavior, while at high temperatures, it predominantly demonstrates expansion failure. This phenomenon can be attributed to the increased brittleness of specimens caused by ice crystals, rendering it more susceptible to brittle failure under shearing forces. These findings signify an enhancement in the mechanical behavior of WCM within the tunnel sidewall under artificial freezing conditions.

Keywords: weakly consolidated mudstone; artificial ground freezing; triaxial shear test; shear strength; water-diversion tunnel

check for updates

Citation: Quan, H.; Zhang, W.; Li, J.; Ru, X.; Zhou, J.; An, R. Enhancing Shear Strength of Weakly Consolidated Mudstone in Water-Diversion Tunnels Through Artificial Ground-Freezing Techniques: An Experimental and Theoretical Study. *Water* **2024**, *16*, 3095. https://doi.org/10.3390/w16213095

Academic Editor: Pankaj Kumar

Received: 27 September 2024
Revised: 22 October 2024
Accepted: 25 October 2024
Published: 29 October 2024

Copyright: © 2024 by the authors. Licensee MDPI, Basel, Switzerland. This article is an open access article distributed under the terms and conditions of the Creative Commons Attribution (CC BY) license (https://creativecommons.org/licenses/by/4.0/).

1. Introduction

With the rapid advancement of China's economy and society, there has been a surge in the development of water conservancy, transportation, and other infrastructures [1,2]. In recent years, with the continuous implementation of the strategy for hydropower energy development in China, there has been a gradual increase in the construction of hydropower stations and water-diversion projects under poor geological conditions [3]. Inevitably,

the construction of water-diversion tunnels is occurring frequently under unfavorable geological conditions, leading to substantial engineering hazards and risks [4,5]. Among these challenges, fault fracture zones represent the most prevalent adverse geological phenomenon. As a result, during tunnel construction, engineering accidents such as collapse, water outbursts, and mud outbursts are prone to occur, resulting in significant losses for construction efforts [6].

The artificial ground-freezing (AGF) method involves artificially freezing the weak rock and soil to achieve a solid state, thereby altering the physical and mechanical properties [7]. This technology has a broad range of applications in the fields of civil engineering, water conservancy, and mining engineering, particularly in addressing construction challenges under unique geological conditions such as groundwater and fault fracture zones [8,9]. Refrigeration equipment, such as liquid nitrogen or refrigerant, is employed in AGF construction to lower the temperature of the earth, resulting in the solidification of water and the formation of a frozen wall [10]. As the temperature decreases in this process, the water undergoes a phase transition from liquid to solid, resulting in substantial alterations in the physical and mechanical characteristics of the geomaterials [11]. In real engineering, the AGF method can be utilized for foundation-pit excavation, levee reinforcement, and water conveyance tunnel excavation to enhance project stability and safety [12–15]. Artificial frozen geomaterials are commonly utilized in laboratory settings to conduct experimental research aimed at investigating their physical and mechanical properties, as well as their potential applications in engineering.

The water-diversion tunnel, as a common structure in hydroelectric engineering, may face challenges during construction due to poor geological conditions [16]. Weakly consolidated mudstone (WCM), as a special rock material in tunnel sidewall, exhibits complex mechanical properties and components with a changeable structure that is significantly influenced by temperature shifts [17]. WCM is a discontinuous medium with a complex formation process, a high clay mineral content, a low strength, a strong plasticity, and susceptibility to environmental influences [18,19]. It exhibits weak structural surfaces including primary fractures, joints, and fissures [20]. Artificial freezing is a highly effective technique for treating mudstone, particularly in the context of tunnel construction [21]. Under freezing conditions, pore water within the geomaterials can freeze and form ice crystals, which increases cementation and friction between rock grains, thereby improving its shear strength [22,23]. Therefore, the mechanical properties of the surrounding rocks within the tunnel sidewall enhance under short-term freezing conditions [24]. However, this enhanced brittleness makes the surrounding rock more susceptible to brittle failure when disturbed by external forces leading to obvious shear planes and cracks. The application of the AGF method in the formation of friable rocks is challenging [25–27]. Currently, there is limited research on the mechanical behavior of WCM within tunnel sidewalls under freezing conditions, especially regarding changes in shear strength under different temperatures and confining pressures, thus necessitating further investigation.

Under low temperatures, the thermal and mechanical characteristics of the surrounding rocks within the tunnel sidewall are susceptible to fluctuations in temperature, resulting in heightened fragility and strength levels [28]. Consequently, this renders the structure more vulnerable to instability under external loads or disturbances, despite its increased compressive strength [29]. The research indicates that the alteration of freezing temperature not only impacts the shear strength of mudstone, but also modifies its failure mode. For instance, in frozen conditions, there is a significant increase in the number of fracture cracks of mudstone, leading to an overall deterioration in stability [30]. These alterations pose greater demands on tunnel design and safety assessment, particularly under poor geological conditions where the influence of freezing on the stability of surrounding rock must be carefully considered [31]. Therefore, it is crucial to investigate the strength and stability of WCM under freezing action for ensuring the safe construction of hydraulic structures.

Currently, there has been some advancement in the investigation of the artificial freezing impact on weakly consolidated rocks. CHRIST et al. [32] conducted a comprehensive

physical and mechanical investigation to determine the compressive strength and microscopic morphology evolution of frozen soils. The study revealed that low-temperature freezing can enhance strength properties, while multiple freeze–thaw cycles may have a detrimental impact on mechanical behavior. PIMENTEL et al. [33] conducted an experimental study on the effect of initial water content on the physical and mechanical properties of soft rock and the rule of water migration during an artificial freezing process. FU et al. [34] conducted an analysis on the variation of physical and mechanical parameters of completely weathered granite under different freezing conditions and provided a comprehensive summary of the shear modes and failure types. AN et al. [35] demonstrated that the shear strength, internal friction angle, and cohesion of mudstone exhibit a significant increase under artificial freezing conditions, resulting in the enhanced stability of the weathered-granite formation in a low-temperature environment. The thermal conditions play a crucial role in shaping the microstructure of frozen rocks and soils [36]. The shear strength and deformation properties exhibit significant variability in response to changes in cooling temperatures [37]. Although the thermal effect of frozen soil has been understood, the relationship between shear strength and microstructure under different temperatures still needs to be further understood. Existing research indicates that an in-depth study of the mechanical behavior effects of WCM under different cooling temperatures can effectively improve the safety and economic benefits of engineering construction.

Through a series of well-designed systematic experimental studies, this study investigated the specific effects of various freezing conditions on the shear strength of WCM in the tunnel sidewall. Based on the results of the mechanical tests under varying temperature and confining pressure conditions, this study successfully unveiled the evolution of its shear strength and deeply investigated the internal failure mechanism responsible for such changes in shear strength. These findings deepened our understanding of the mechanical behavior of WCM under artificial freezing conditions.

2. Materials and Methods

2.1. Testing Materials

The experimental materials were derived from a hillside in Liaodong City, Liaoning Provence, northeast China, as depicted in Figure 1. The sampling site belongs to a seasonally frozen region with a complex topography with elevations as high as 820 m and abundant rainfall, and where the climate conditions are harsh, with cold winters and short, cool summers. The terrain is complex, including mountains, valleys, and rivers. In order to reduce sampling disturbance, a medium core drill is used to automatically collect natural rock samples in this environment. Figure 2 provides a detailed depiction of the sampling site environment, showcasing the distinct surface appearance and unique microtopography of the mudstone. Geological investigation has confirmed that the sample originated from the ancient Permian formation, with its appearance displaying a sharp yellow-to-brown appearance attributed to the abundant iron oxides present, particularly an extensive presence of hematite. WCM demonstrates moderate strength and favorable plasticity; however, it is critical to note that their mechanical properties exhibit strong sensitivity to changes in ambient temperature.

During the sampling process, it was observed that the groundwater level was shallow, leading to a high natural moisture content of WCM at 23.7%. This characteristic significantly influenced the engineering properties of the WCM. To gain further insight into the physical properties of the WCM, comprehensive in-lab physical property tests were conducted and the results are summarized in Table 1. The data revealed that the relative density of the weakly consolidated mudstone was 2.73, with a dry density of 1.42 g/cm^3 and a void ratio of 0.63. The mudstone exhibits a high liquid limit of 52.1%, indicating its significant plasticity and deformation potential. The main mineral composition included feldspar (19.2%), quartz (26.5%), kaolinite (25.9%), illite (17.4%), and montmorillonite (9.7%), collectively contributing to its complex mineralogical characteristics (Figure 3b). To accurately analyze the particle composition of weakly consolidated mudstone, a comprehensive particle size

analysis was conducted following the ASTM standard of screening method [38]. The particle grading curves depicted in Figure 3b provide an intuitive representation of the grain size distribution within the mudstone. It is evident from these curves that the mudstone predominantly consists of two distinct ranges of silt and clay particles, thereby holding significant implications for assessing its engineering performance and potential mechanical behavior.

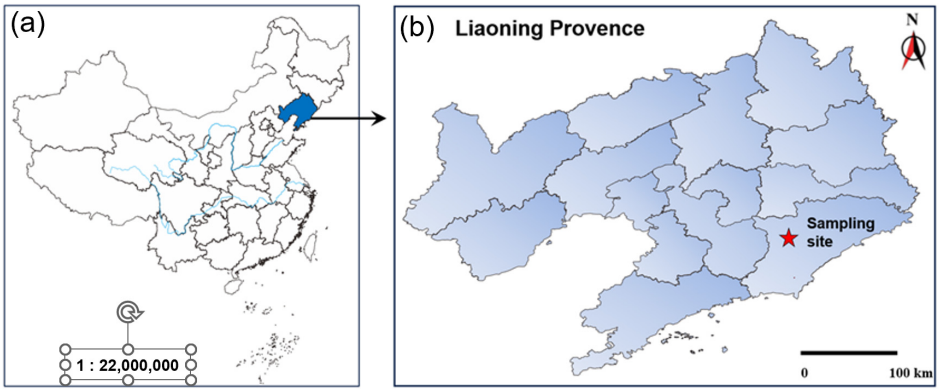


Figure 1. Geographic location of the sampling site: (**a**) Map of China, (**b**) Map of Liaoning Provence.

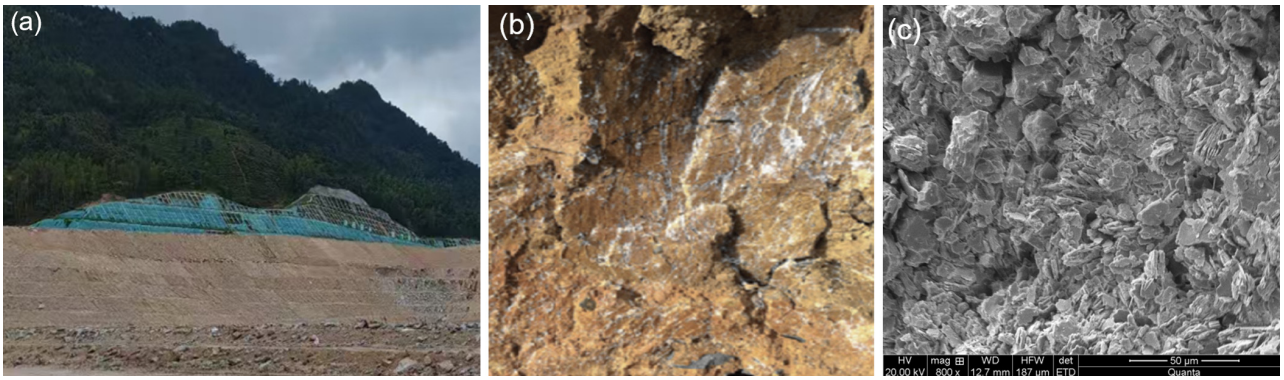


Figure 2. Sampling site, photo, and microstructure of the weakly consolidated mudstone used in this study: (**a**) engineering site; (**b**) appearance of samples; (**c**) SEM image with 800× magnification.

Table 1. Physical and chemical properties of the mudstone.

Physical Property	Dry Density (g/cm^3)	Relative Density	Moisture Content (%)	Void Ratio	Liquid Limit (%)	Plastic Limit (%)
Value	1.42	2.73	23.7	0.63	52.1	19.3

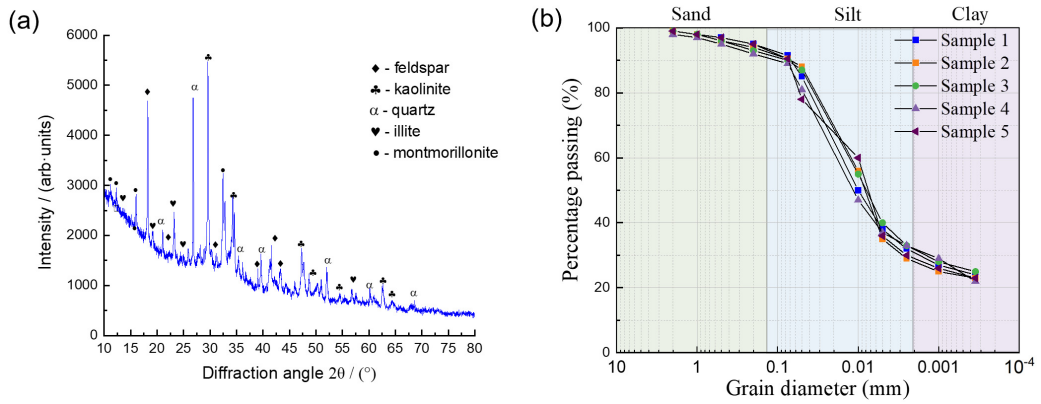


Figure 3. Mineral and grain composition of weakly consolidated mudstone: (**a**) X-ray diffraction spectrum and (**b**) particle size distribution.

2.2. Sample Preparation

Prior to testing, undisturbed cubic samples of WCM were carefully extracted from wooden containers and their protective covering was removed. Subsequently, the samples were precisely divided into cylindrical segments measuring 50 mm in diameter and 100 mm in height. It is crucial during this process to ensure the accuracy of blade sharpness and cutting angles in order to maintain the integrity of the specimens. Upon completion of segmentation, these cylindrical specimens were grinded and polished to achieve a smooth exterior. Subsequently, the finalized cylindrical specimens (Figure 4a) were stored in a controlled environment that is dry, cool, and shielded from direct sunlight and abrupt temperature changes to ensure the accuracy and reliability of the subsequent experimental results.

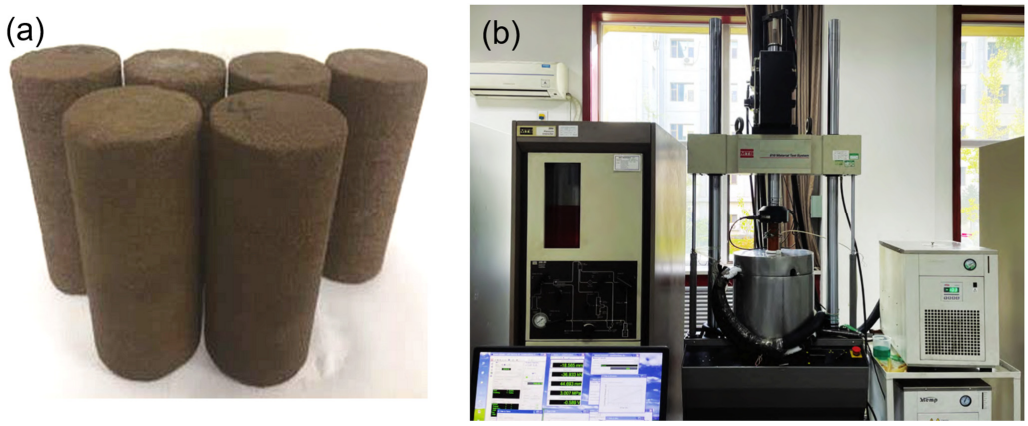


Figure 4. Experimental specimen and device: (**a**) the tested WCM specimens and (**b**) GDS triaxial testing system.

2.3. Triaxial Shear Tests

The experiment utilized the high-pressure frozen soil dynamic and static triaxial testing system manufactured by the GDS Company (Figure 4b). The test system comprises a pressure chamber, loading frame, pressure controller, and temperature control system. Notably, the maximum volume of the pressure chamber is 10 MPa, and the maximum load of the axial load sensor is 32 kN, meeting the specific requirements of this experiment. According to the uncertainty requirement of the experiment, several samples were taken for triaxial shear strength test. The triaxial shear test in this study included two specimens in each testing group. The surface of the specimen was smooth and free from cracks. This step reduced internal stress and potential damage to the specimen, ensuring more accurate results in subsequent experiments. The specimens were exposed to ambient freezing conditions that did not affect their moisture content before testing. The experiment was conducted in consolidated undrained shear mode with four different consolidated confining pressures set under varying freezing conditions. Upon reaching the target temperature, each specimen was allowed to freeze completely and reach thermal equilibrium for 24 h before undergoing shear testing to prevent any warming or temperature fluctuations. Precise control of the loading rate was crucial. The appropriate loading rate is determined through preliminary experimentation. Computerized data collection automatically recorded stress and strain test results along with documenting failure modes when reaching peak stress levels and stabilizing after loading cessation.

To minimize the impact of temperature variations on experimental outcomes, it was essential to maintain temperature fluctuations within ± 0.2 °C. Before proceeding with the formal experiment, the specimen was placed in a low-temperature environment for pre-cooling treatment. The pre-cooling treatment duration was meticulously extended to guarantee uniform internal specimen temperature distribution. This controlled cooling rate is vital to avoid creating excessive temperature gradients within the specimen, thereby achieving a uniform freezing process. In triaxial shear experiments, thermal insulation is

utilized to wrap the experimental equipment, providing an extra layer of protection against temperature fluctuations. By meticulously following these steps, the impact of temperature fluctuations on the results of mechanical experiments can be significantly minimized.

3. Results

3.1. Failured Mode and Stress–Strain Curves

Figure 5 illustrates an instance of shear failure patterns observed in frozen specimens of WCM during triaxial shear testing. Under low confining pressures, the specimens exhibited minimal visible fracturing upon failure; however, there were notable alterations in its internal structure, accompanied by localized yielding and flow phenomena. Additionally, the frozen WCM specimens demonstrated dilatancy effects during failure. Under high confining pressures, the specimens exhibited distinct shear zone failure, resulting in the formation of prominent shear planes or cracks that traversed the entire sample along the direction of shearing, while maintaining intact ends. The rock sample was moving within the shear zone at a 45° angle relative to the axial direction, indicating significant deformation and major cracks within the WCM. The specimen displayed bending or folding along the axial surface, with evident sliding marks within the shear zone and shear shrinkage properties. As the freezing temperature dropped, the brittleness response characteristics of the WCM specimens became increasingly pronounced. Furthermore, the dilatancy phenomenon also intensified when the specimens were damaged, resulting in a relatively flat rupture surface. This phenomenon is partly attributed to the substantial increase in specimen hardness during the artificial freezing process, which effectively restricts the surface bending of the sample under ultimate stress. Summarily, the failure characteristics of specimens during triaxial shear tests are closely correlated with the physical and mechanical properties of WCM. These failure characteristics serve as a crucial basis for comprehending the mechanical behavior and failure mechanism. In the case of frozen mudstone, ambient temperature significantly influences the shear failure mode.

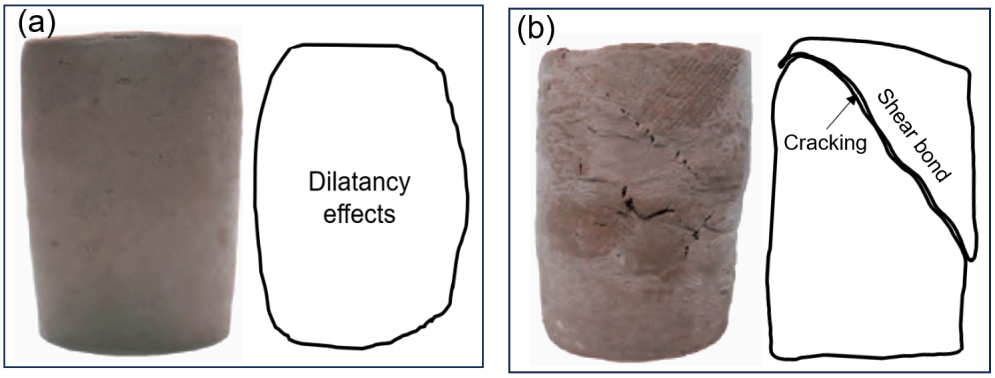


Figure 5. Stress–strain curves of mudstone under different freezing conditions: (**a**) low confining pressure and (**b**) high confining pressure.

Figure 6 illustrates the changes in shear strength under various conditions and effectively reveals how the mechanical properties are influenced by both confining pressure and freezing temperature. It is observed that the stress–strain curves exhibit a consistent and smooth increasing trend regardless of changes in freezing temperature or adjustments in confining pressure. Specifically, as axial strain gradually increases, deviational stress demonstrates a continuous and stable upward trend without any significant softening phenomenon or plateau throughout the entire process. This phenomenon indicates the excellent continuity and consistency of frozen specimens during shearing. For example, at a temperature of 0 °C, the shear strength significantly increased from 1.85 MPa to 6.92 MPa, achieving an increase of 274.1% when the effective confining pressure was raised from 1 MPa to 4 MPa. This can be attributed to the significant enhancement in interaction force between rock grains under elevated confining pressure conditions, thereby promoting the

loading capacity of WCM specimens. Further data analysis indicates that the increase in effective confining pressure has a significant impact on the compressive strength. Specifically, the enhancement of confining pressure directly results in a noticeable improvement in shear strength, demonstrating the positive influence of confining pressure on material shear properties. The decrease in ambient temperature, as another crucial variable, also substantially enhances strength. Additionally, high confining pressure led to a more substantial increase in the strength of frozen specimens of WCM. This trend of increasing strength becomes more pronounced at lower ambient temperatures, highlighting the substantial regulatory effect of temperature on the mechanical properties of frozen WCM specimens.

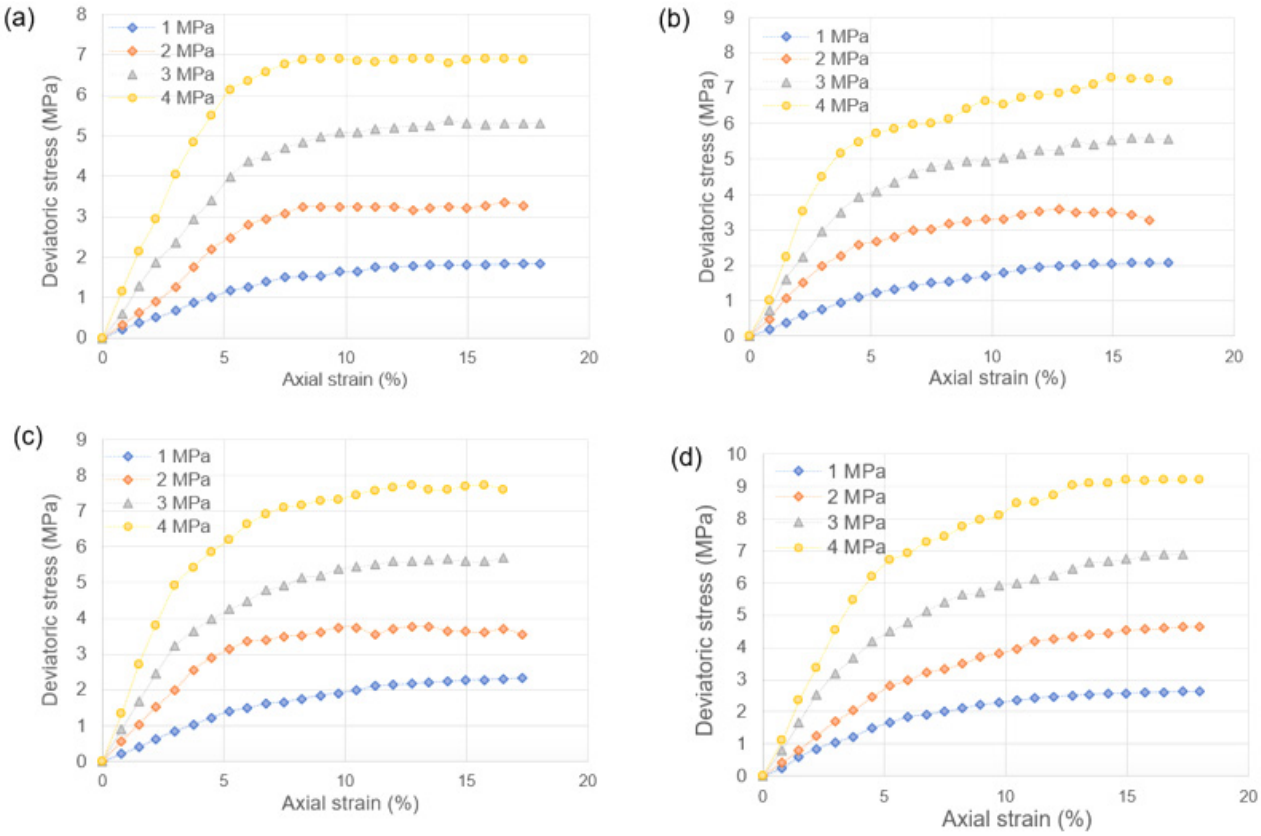


Figure 6. Stress–strain curves of the WCM under different confining pressures at a temperature of: (**a**) 0 °C, (**b**) −5 °C, (**c**) −10 °C, and (**d**) −20 °C.

3.2. Evolution of Shear Strength and Yield Strain

Due to external loading, the deviatoric stress accumulates within it in a corresponding condition. In the initial phase, the mudstone distinctly demonstrates elastic behavior characteristics, signified by a rigorously linear correlation between stress and strain, thereby indicating that the specimen is residing in the stage of elastic deformation. As axial stress reaches a critical level, the deformation mechanism experiences a fundamental shift from elastic to plastic deformation, resulting in the corresponding yield strain. This transition signifies a significant change in the mechanical behavior under axial stress and has important implications for its mechanical properties. To further investigate the specific impacts of various freezing conditions on the shear characteristics of WCM specimens, this study systematically examined the variations in shear strength (Figure 7) and yield strain (Figure 8) with changes in ambient temperature and effective confining pressure. According to the classical theoretical basis of rock and soil mechanics, the initial yield strain is defined as the strain value corresponding to the initial yield (or elastic limit point) on the stress–strain curve.

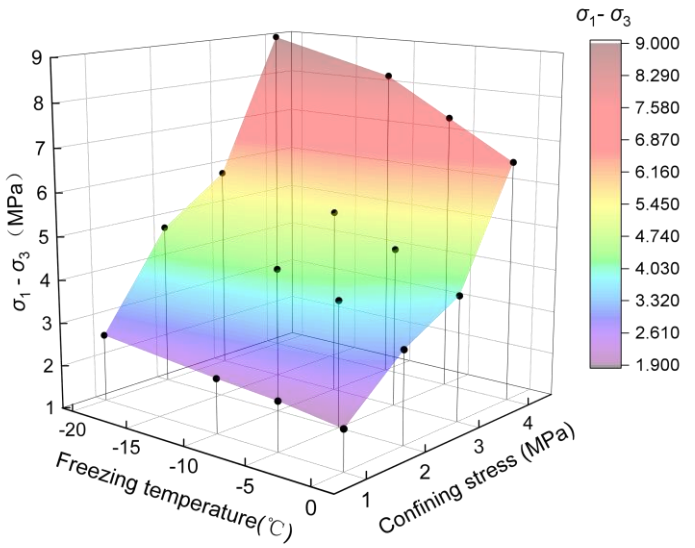


Figure 7. Shear strength with different freezing temperatures and confining pressures.

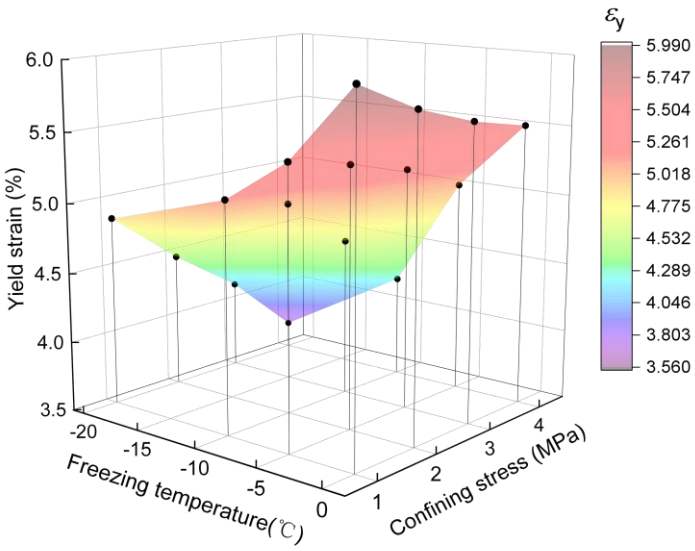


Figure 8. Yield strain with different freezing temperatures and confining pressures.

The results presented in Figure 7 demonstrate that the reduction in freezing temperature and the increase in effective confining pressure contribute to an enhancement of shear strength (σ_1–σ_3) in the specimen. However, a decrease in ambient temperature leads to increased brittleness of the frozen specimens, as evidenced by a stress–strain curve showing minimal strain post-failure and rapid decline after reaching peak stress, with a gradual transition from ductile to brittle failure. Additionally, Figure 8 illustrates that at a confining pressure of 4 MPa and freezing temperature of −20 °C, the yield strain ε_y for the frozen clay sample is only 3.60%. The analysis indicates that the alteration of the stress–strain curve in the specimens under low-temperature conditions is primarily influenced by the presence of frozen water and changes in the internal structure. As temperatures decrease below 0 °C, pore water within the mudstone begins to freeze, forming ice crystals with heightened strength and stiffness. This results in an elevation of both peak stresses and initial slope on the stress–strain curve at lower temperatures. Furthermore, frozen water forms ice crystals that function as a cementation agent, effectively binding together rock particles and subsequently enhancing shear strength and elastic modulus of the specimens. Furthermore, as the freezing temperature decreases, water freezing in the pores and micro-fissures within the mudstone result in a reduction in pore volume and healing of fissures, thereby enhancing the overall strength of the specimens. In addition, the presence of ice crystals

reduces relative sliding between rock particles, leading to less plastic deformation at low temperatures and exhibiting pronounced brittleness characteristics. The ice formation significantly impacts its yield strain [33]. Generally, as freezing temperature decreases and ice content increases, yield strain decreases due to reduced friction between particles caused by ice lens skeleton action and decreased plastic deformation. The presence of ice crystals within the pores can significantly contribute to the enhancement of shear strength in frozen mudstone by increasing cohesion and internal friction angles. However, it is crucial to acknowledge the potential for ice-crystal melting or recrystallization within the pores when the confining pressure exceeds a certain threshold, which may hinder the enhancement of shear strength as confining pressure rises [26].

4. Discussion

Figure 9 illustrates the variation in shear strength index of the WCM specimens under different testing conditions. In this study, we utilized functions within the Origin 2021 software to perform statistical data fitting. This process entails the calculation of model parameters in order to optimize the fit with the data. The efficacy of the model's fit was assessed through computation of the coefficient of determination index (R^2). It is evident from Figure 9 that the cohesion and internal friction angles both increase as the freezing temperature decreases. The relationship between cohesion, internal friction angle, and freezing temperature is studied and analyzed based on the function fitting of exponential functions. The specific relationships are shown in Equations (1) and (2).

$$c(t) = -572.8e^{-0.108t} + 1580.16 \quad (1)$$

$$\varphi(t) = -16.98e^{-0.112t} + 61.21 \quad (2)$$

where t refers to the freezing temperature and c and φ are the cohesion (c) and internal friction angle, respectively.

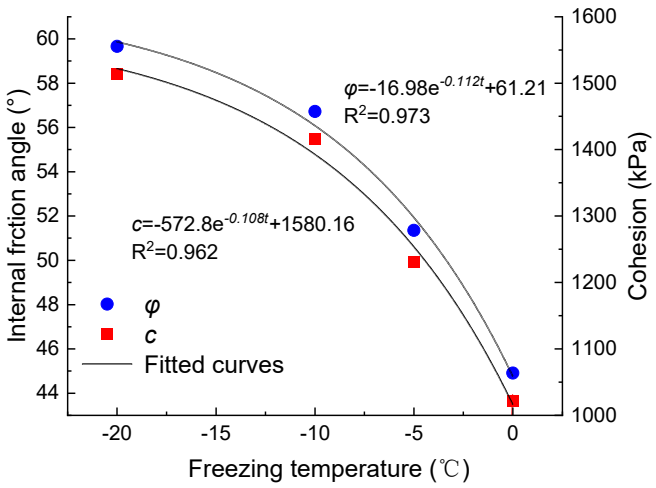


Figure 9. Relationship between cohesion, internal friction angle, and freezing temperatures.

As shown in Figure 10, the liquid water in pores underwent a freezing process and transformed into ice crystals. These ice crystals served as natural adhesives that significantly enhanced the friction between rock particles and played a crucial cementing role. Furthermore, freezing caused the pore water to convert into ice, further reinforcing the internal structure of WCM. By strengthening the mechanical interlocking effect between particles, it effectively increased the internal friction angle. This phenomenon was closely related to enhancing particle friction and stabilizing mudstone microstructure. The freezing process also causes the pore water to change into ice, further strengthening the internal structure of the clay and effectively increasing the internal friction angle by strengthening

the mechanical bite effect between the particles. On the other hand, the phenomenon that the cohesion increased with the decrease in freezing temperature can also be attributed to the enhanced cementation and occlusion of ice crystals between rock and clay particles. The ice crystals played a crucial role in enhancing the bond between clay particles as a binder, and also contributed to an increase in contact pressure among the particles through volumetric expansion during their formation, thereby leading to improved cohesive force [39]. However, cracks formed due to temperature gradients and water migration under extreme freezing temperatures. The expansion of these cracks weakened the specimen's stability and mechanical behavior, reducing cohesion and internal friction angle. Hence, the relationship between cohesion and temperature, as well as internal friction angle and temperature, were described by an exponential function.

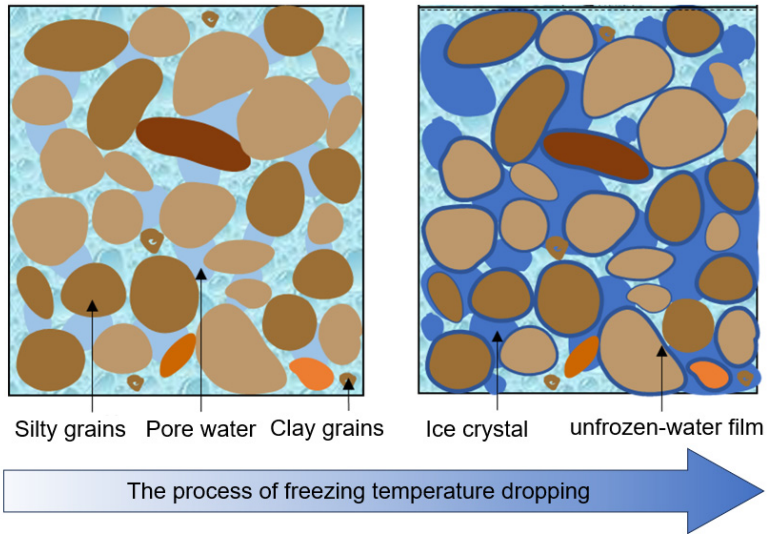


Figure 10. Diagram of changing microstructure in weakly consolidated mudstone during the freezing process.

By comparing the results of laboratory experiments, it was found that the stress–strain curves of frozen WCM in this study respond to temperature and confining pressure similarly to those of frozen soil [40]. When the freezing temperature was low, frozen soil showed significant brittleness, and cracks occurred easily during loading. On the contrary, when the temperature was higher, the sample exhibited plastic characteristics. The failure pattern of the WCM specimen was found to be markedly affected by temperature, with a notable occurrence of shear zone failure at lower temperatures and a prevailing tendency towards swelling failure at higher temperatures. During the loading process, the ice lens in the specimens had a process of melting and refreezing. Under high confining pressure conditions, the bonding effect of ice crystals is strengthened, which inhibits the expansion of cracks in the specimen. As can be observed in Figure 11, WCM under low confining pressures exhibited plastic failure characteristics with observable failure bands, whereas the ice crystals in WCM only carried a portion of the load. The WCM specimen during triaxial loading first displayed a characteristic of shrinkage and then dilatancy under such conditions. Under high confining pressure, distinct failure cracks and oblique shear zones were observed on the bulging side of the specimen. This phenomenon can be attributed to the stress concentration and grain breakage of ice crystals, which enhanced the brittleness of frozen specimens, thereby making it more prone to brittle failure when subjected to high confining pressure during triaxial loading [41]. During the freezing process, there was a possibility for pore water pressure to become concentrated in specific areas, resulting in stress concentration phenomena. This phenomenon had a substantial influence on mechanical properties, including shear strength, frost heave force, crack propagation, and brittleness.

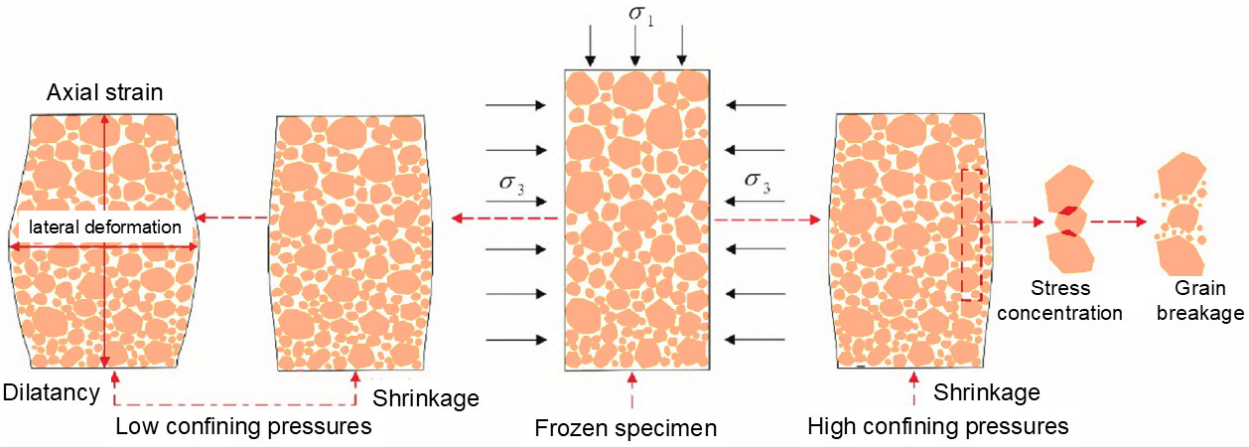


Figure 11. Stress state diagram of weakly consolidated mudstone under triaxial loading.

The conventional approach proposed by previous scholars primarily relies on uniaxial compression experiments to characterize the artificial frozen effects, with the main indices obtained being uniaxial compressive strength and elastic modulus [38,42]. For instance, it was observed that freezing temperature and moisture content exert significant effects on the mechanical parameters [15]. The frozen triaxial shear test was employed to investigate the enhancement of WCM under artificial freezing conditions. This study revealed that the triaxial shear test can more comprehensively and accurately reflect the influencing factors of artificial freezing conditions on WCM. Furthermore, different freezing factors were taken into consideration during the test, providing a more reliable reference for tunnel construction using freezing methods.

In conclusion, the macroscopic distinctions between WCM specimens under artificial frozen state and conventional state suggest that the alterations in mudstone are more intricate, posing challenges for the application of traditional theories of rock mechanics in analyzing its mechanical behavior. Through the analysis of the shear strength of WCM during AGF construction under varying combined conditions of temperature and confining pressure, the evolution of its shear strength and the underlying mechanisms governing its failure were clarified. This comprehensive investigation not only enhanced our comprehension of the mechanical behavior of mudstone in complex environmental settings but also provided theoretical guidance for subsequent research and practical applications.

5. Conclusions

Based on the results of triaxial shear tests, this study examined the impact of freezing temperatures and confining pressures on the mechanical characteristics of the WCM in a water-diversion tunnel. The main conclusions are as follows:

(1) As the freezing temperature decreases from 0 °C to −20 °C, there is an increase in cohesion and internal friction angle from 1012 kPa to 1425 kPa, accompanied by a rise in the internal friction angle from 43.2° to 58.2°. The exponential function is capable of delineating the correlation between cohesion, internal friction angle, and freezing temperature. A notable enhancement in the shear strength of WCM specimens is observed under AGF conditions at various levels of confined pressures, indicating a significant impact on the mechanical behavior.

(2) The yield strain is reduced due to decreased grain friction caused by the ice lens skeleton and lower plastic deformation, attributed to declining freezing temperatures and increasing ice content. As the freezing temperature decreases, the frozen specimen of WCM undergoes a transition from plastic failure to brittle fracture, resulting in the deformation of dilatancy failure shifting towards shrinkage failure.

(3) In low-freezing environments, the influence of confining pressure on the shear strength becomes more pronounced. Notably, high confining pressure leads to a substantial increase in the strength of frozen specimens of WCM. This can be attributed to ice crys-

tals filling cracks within the frozen WCM under combined low temperature and high confining pressure conditions, thereby reducing crack expansion and deformation while enhancing overall strength.

(4) The failure pattern of the WCM specimen is significantly influenced by freezing temperatures, with significant shear zone failure observed at low freezing temperatures for WCM, and dominant swelling failure at high temperatures. This can be attributed to the presence of ice crystals increasing the brittleness of WCM, making it more susceptible to brittle failure during triaxial loading. The findings provide strong technical support for the application of the AGF method in the construction of water-diversion tunnels.

Author Contributions: Conceptualization, J.L.; methodology, H.Q. and W.Z.; formal analysis, X.R.; validation, H.Q.; investigation, R.A. and J.Z.; resources, X.R.; writing—original draft preparation, H.Q.; writing—review and editing, J.L. and R.A.; supervision, J.L.; funding acquisition, J.L. All authors have read and agreed to the published version of the manuscript.

Funding: This research was funded by the National Natural Science Foundation of China (41662013) and the Gansu Provincial Science and Technology Plan Project (No. 21JR7RA541).

Data Availability Statement: Data are available upon reasonable request.

Acknowledgments: The authors thank the anonymous reviewers and editors for their comments on this manuscript.

Conflicts of Interest: Wenzhi Zhang is employed by Qiantang River Administration Design Institute Co., Ltd., Junjie Li and Xiaoxue Ru are employed by Zhejiang Design Institute of Water Conservancy and Hydroelectric Power Co., Ltd., and Jingbo Zhou is employed by the company Zhejiang Engineering Survey and Design Institute Group Co., Ltd. The remaining authors declare that the research was conducted in the absence of any commercial or financial relationships that could be construed as a potential conflict of interest.

References

1. Poraj-Górska, A.I.; Zarczynski, M.J.; Ahrens, A.; Enters, D.; Weisbrodt, D.; Tylmann, W. Impact of Historical Land Use Changes on Lacustrine Sedimentation Recorded in Varved Sediments of Lake Jaczno, Northeastern Poland. *CATENA* **2017**, *153*, 182–193. [CrossRef]
2. Wang, Y.; Dong, Y.; Su, Z.; Mudd, S.M.; Zheng, Q.; Hu, G.; Yan, D. Spatial Distribution of Water and Wind Erosion and Their Influence on the Soil Quality at the Agropastoral Ecotone of North China. *Int. Soil. Water. Conserv. Res.* **2020**, *8*, 253–265. [CrossRef]
3. Yuan, P.; Zhang, W.; Shang, X.; Pu, Y. Intrusion Event lassification of a Drainage Tunnel Based on Principal Component Analysis and Neural Networking. *Water* **2024**, *16*, 2409. [CrossRef]
4. Feng, A.; Zhu, Z.; Zhu, X.; Zhang, Q.; Yan, E.; Li, Z.; Guo, Y.; Singh, V.P.; Zhang, K.; Wang, G. Impacts of Water Diversion Projects on Vegetation Coverage in Central Yunnan Province, China (2017–2022). *Remote Sens.* **2024**, *16*, 2373. [CrossRef]
5. Kong, Z.; Ling, H.; Deng, M.; Han, E.; Yan, J.; Deng, X.; Wang, Z.; Ma, Y.; Wang, W. Past and projected future patterns of fractional vegetation coverage in China. *Sci. Total Environ.* **2023**, *902*, 166133. [CrossRef]
6. Hu, X.; Wu, Y.; Li, X. A field study on the freezing characteristics of freeze-sealing pipe roof used in ultra-shallow buried tunnel. *Appl. Sci.* **2019**, *9*, 1532. [CrossRef]
7. Jones, J.S. State-of-the-art report–Engineering practice in artificial ground freezing. *Eng. Geol.* **1981**, *18*, 313–326. [CrossRef]
8. Weisbrod, N.; Niemet, M.R.; Rockhold, M.L.; McGinnis, I.; Selker, J.S. Migration of saline solutions in variably saturated porous edia. *J. Contam. Hydrol.* **2004**, *72*, 109–133. [CrossRef]
9. Hu, X.; Fang, T. Numerical simulation of temperature field at the active freeze period in tunnel construction using freeze-sealing pipe roof method. Tunneling and underground construction. In Proceedings of the Geo-Shanghai 2014, Shanghai, China, 26–28 May 2014; pp. 731–741.
10. Cui, Z.D.; Zhang, L.J.; Xu, C. Numerical simulation of freezing temperature field and frost heave deformation for deep foundation pit by AGF. *Cold Reg. Sci. Technol.* **2023**, *213*, 103908. [CrossRef]
11. Russo, G.; Corbo, A.; Cavuoto, F.; Autuori, S. Artificial ground freezing to excavate a tunnel in sandy soil. Measurements and back analysis. *Tunn. Undergr. Space Technol.* **2015**, *50*, 226–238. [CrossRef]
12. Hong, Z.; Zhang, J.; Han, L.; Wu, Y. Numerical Study on Water Sealing Effect of Freeze-Sealing Pipe-Roof Method Applied in Underwater Shallow-Buried Tunnel. *Front. Phys.* **2022**, *9*, 794374. [CrossRef]

13. Joudieh, Z.; Cuisinier, O.; Abdallah, A.; Masrouri, F. Artificial Ground Freezing—On the Soil Deformations during Freeze-Thaw Cycles. *Geotechnics* **2024**, *4*, 718–741. [CrossRef]
14. Niu, Y.; Hong, Z.Q.; Zhang, J.; Han, L. Frozen curtain characteristics during excavation of submerged shallow tunnel using *re*Freeze-Sealing Pipe-Roof method. *Res. Cold Arid. Reg.* **2022**, *14*, 267–273.
15. Alzoubi, M.A.; Xu, M.; Hassani, F.P.; Poncet, S.; Sasmito, A.P. Artificial ground freezing: A review of thermal and hydraulic aspects. *Tunn. Undergr. Space Technol.* **2020**, *104*, 103534. [CrossRef]
16. Li, T.; Zhang, Q.; Wang, G.; Singh, V.P.; Zhao, J.; Sun, S.; Wang, D.; Liu, T.; Duan, L. Ecological degradation in the Inner Mongolia reach of the Yellow River Basin, China: Spatiotemporal patterns and driving factors. *Ecol. Indic.* **2023**, *154*, 110498. [CrossRef]
17. Wang, S.; Han, L.; Zhang, S.; Wang, H. Structure Restrengthening Process and Mechanical Properties of Damaged Weakly Cemented Mudstone. *Sustainability* **2023**, *15*, 9148. [CrossRef]
18. Dessouki, M.; Hathon, L.; Myers, M. Permeability and Porosity Modelling for Resedimented Mudrocks—Applications for Compaction Dominated Mudrock Systems. *Mar. Pet. Geol.* **2021**, *128*, 104945. [CrossRef]
19. Chen, Z.; Liu, H.; Zhu, C.; Ma, S.; Hang, Y.; Luo, W. Seepage Characteristics and Influencing Factors of Weakly Consolidated Rocks in Triaxial Compression Test under Mining-Induced Stress Path. *Minerals* **2022**, *12*, 1536. [CrossRef]
20. Guo, S.R.; Pu, H.; Yang, M.S.; Liu, D.; Sha, Z.H.; Xu, J.C. Study of the Influence of Clay Minerals on the Mechanicaland Percolatior Properties of Weakly Cemented Rocks. *J. Geofluids* **2022**, *2022*, 1712740.
21. Yao, C.; Zhong, H.; Zhu, Z. Development of a Large Shaking Table Test for Sand Liquefaction Analysis. *Lithosphere* **2024**, *2*, 137. [CrossRef]
22. Alzoubi, M.A.; Sasmito, A.P.; Madiseh, A.; Hassani, E.P. Intermittent freezing concept for energy saving in artificial ground freezing systems. *Energy Procedia* **2017**, *142*, 3920–3925. [CrossRef]
23. Tounsi, H.; Rouabhi, A.; Jahangir, E. Thermo-hydro-mechanical modeling of artificial ground freezing taking into account the salinity of the saturating fluid. *Comput. Geotech.* **2020**, *119*, 103382. [CrossRef]
24. Xie, S.; Lin, H.; Chen, Y.; Yong, R.; Xiong, W.; Du, S. A damage constitutive model for shear behavior of joints based on determination of the yield point. *Int. J. Rock Mech. Min. Sci.* **2020**, *128*, 104269. [CrossRef]
25. Lu, Y.; Liu, S.H.; Zhang, Y.G.; Wang, L.J.; Li, Z. Hydraulic conductivity of gravelly soils with various coarse particle contents subjected to freeze–thaw cycles. *J. Hydrol.* **2021**, *598*, 126302. [CrossRef]
26. Tan, X.; Chen, W.; Tian, H.; Cao, J. Water flow and heat transport including ice/water phase change in porous media: Numerical simulation and application. *Cold Reg. Sci. Technol.* **2011**, *68*, 74–84. [CrossRef]
27. Fu, Y.; Hu, J.; Wu, Y. Finite element study on temperature field of subway connection aisle construction via artificial ground freezing method. *Cold Reg. Sci. Technol.* **2021**, *189*, 103327. [CrossRef]
28. Yang, H.; Lei, B.; Xie, L.; Hu, C.; Liu, J. Experimental Study on Water and Salt Migration and the Aggregate Insulating Effect in Coarse-Grained Saline Soil Subgrade under Freeze-Thaw Cycles. *Appl. Sci.* **2024**, *14*, 8970. [CrossRef]
29. Zhang, D.M.; Liu, Y.; Huang, H.W. Leakage-induced Settlement of Ground and Shield Tunnel in Soft Clay. *J. Tongji Univ. (Nat. Sci.)* **2013**, *41*, 1185–1190.
30. Lina, M.G.C.; Siavash, G.; Jean, S. Effect of Anisotropy and Hydro-mechanical Couplings on Pore Pressure Evolution During Tunnel Excavation in Low-permeability Ground. *Int. J. Rock Mech. Min. Sci.* **2017**, *97*, 1–14.
31. Lu, Z.; Xian, S.; Yao, H.; Fang, R.; She, J. Influence of freeze-thaw cycles in the presence of a supplementary water supply on mechanical properties of compacted soil. *Cold Reg. Sci. Technol.* **2019**, *157*, 42–52. [CrossRef]
32. Christ, M.; Kim, Y.-C.; Park, J.-B. The Influence of Temperature and Cycles on Acoustic and Mechanical Properties of Frozen Soils. *KSCE J. Civ. Eng.* **2009**, *13*, 153–159. [CrossRef]
33. Pimentel, E.; Papakonstantinou, S.; Anagnostou, G. Numerical Interpretation of Temperature Distributions from Three Ground Freezing Applications in Urban Tunnelling. *Tunn. Undergr. Space Technol.* **2012**, *28*, 57–69. [CrossRef]
34. Fu, J.; Yang, J.; Zhang, X.; Klapperich, H.; Abbas, S.M. Response of the Ground and Adjacent Buildings Due to Tunnelling in Completely Weathered Granitic Soil. *Tunn. Undergr. Space Technol.* **2014**, *43*, 377–388. [CrossRef]
35. An, R.; Zhang, X.; Kong, L.; Gong, J.; Lei, X. Artificial Ground Freezing Impact on Shear Strength and Microstructure of Granite Residual Soil Under an Extremely Low Temperature. *Front. Earth Sci.* **2021**, *9*, 772459. [CrossRef]
36. Park, J.; Hyun, C.U.; Park, H.D. Changes in microstructure and physical properties of rocks caused by artificial freeze–thaw action. *Bull. Eng. Geol. Environ.* **2015**, *74*, 555–565. [CrossRef]
37. Mousavi, S.Z.S.; Tavakoli, H.; Moarefvand, P.; Rezaei, M. Assessing the effect of freezing-thawing cycles on the results of the triaxial compressive strength test for calc-schist rock. *Int. J. Rock Mech. Min. Sci.* **2019**, *123*, 104090. [CrossRef]
38. *ASTM D7928-21*; Standard Test Method for Particle-Size Distribution (Gradation) of Fine-Grained Soils Using the Sedimentation (Hydrometer) Analysis. American Society for Testing and Materials: West Conshohocken, PA, USA, 2021.
39. Shan, W.; Hou, P.; Xu, G.; Du, H.; Guo, Y.; Zhang, C. Monitoring of the Icing Process and Simulation of Its Formation Mechanism in the Cut Slope of Beihei Highway. *Water* **2024**, *16*, 1851. [CrossRef]
40. Özgan, E.; Serin, S.; Ertürk, S.; Vural, I. Effects of Freezing and Thawing Cycles on the Engineering Properties of Soils. *Soil Mech. Found. Eng.* **2015**, *52*, 95–99. [CrossRef]

41. Gao, H.; An, R.; Zhang, X.; Wang, G.; Liu, X.; Xu, Y. Dynamic evolution of desiccation cracks and their relationship with the hydraulic properties of expansive soil. *Int. J. Geomech.* **2024**, *24*, 04023299. [CrossRef]
42. Wang, X.D.; Li, S.Y.; Sun, Y.F.; Zhang, C.B.; Liu, G.W. Influence of freeze-thaw cycling on the soil mechanical properties of open-pit mine dump under different moisture contents. *Environ. Earth Sci.* **2021**, *80*, 279. [CrossRef]

Disclaimer/Publisher's Note: The statements, opinions and data contained in all publications are solely those of the individual author(s) and contributor(s) and not of MDPI and/or the editor(s). MDPI and/or the editor(s) disclaim responsibility for any injury to people or property resulting from any ideas, methods, instructions or products referred to in the content.